Supplementary Information (SI) for Nanoscale.

SUPPORTING INFORMATION

2D Black Phosphorus as Source of Phosphide Atoms affords Mixed Cobalt Phosphides Clusters Active in the Photocatalytic Hydrogen Evolution

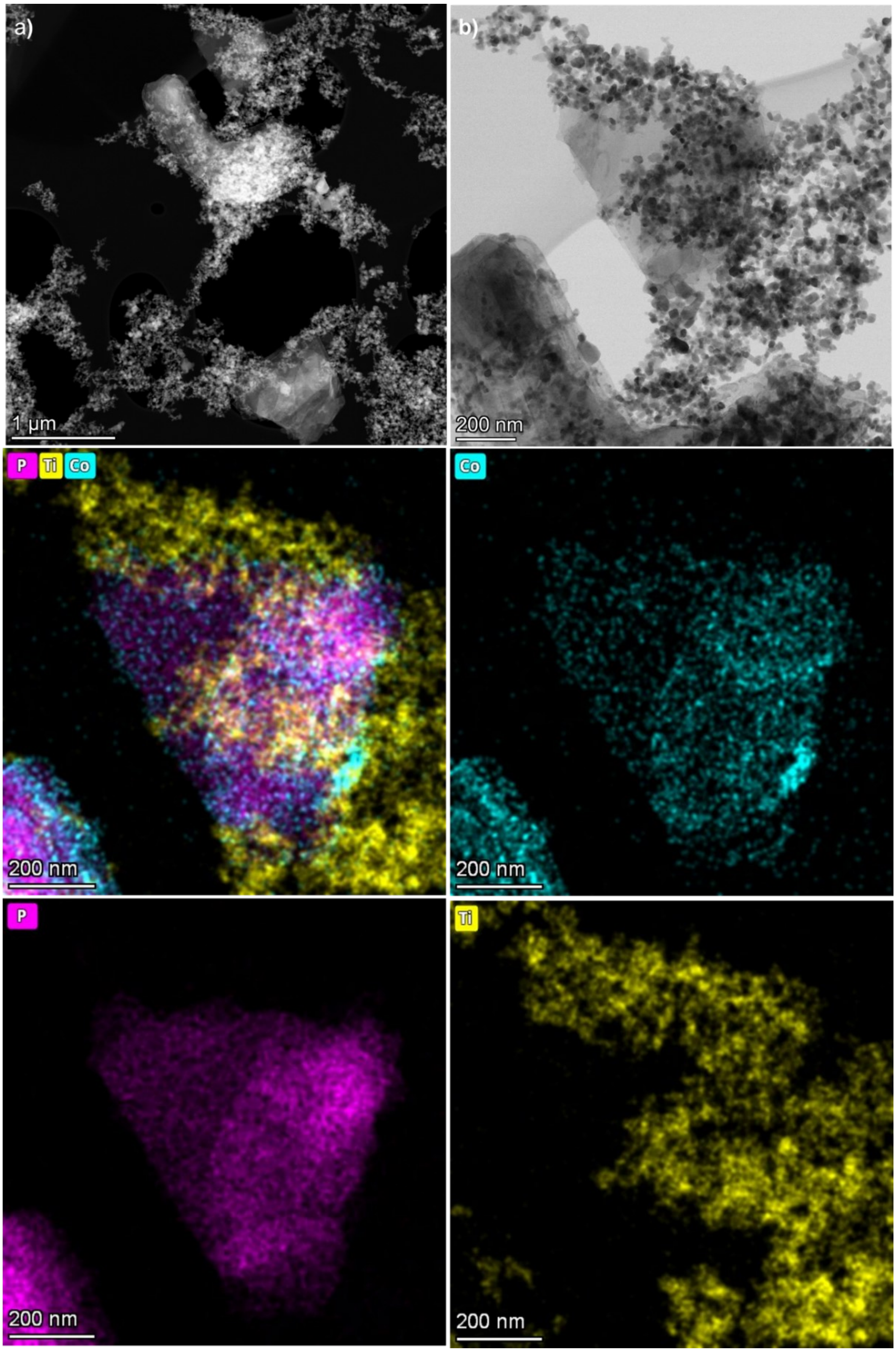

Figure S1. HAADF (a) and BF (b) STEM of TiO_2/BP@CoPx and corresponding EDS elemental mapping. The sample was suspended in acetone and drop casted on holey carbon grid.

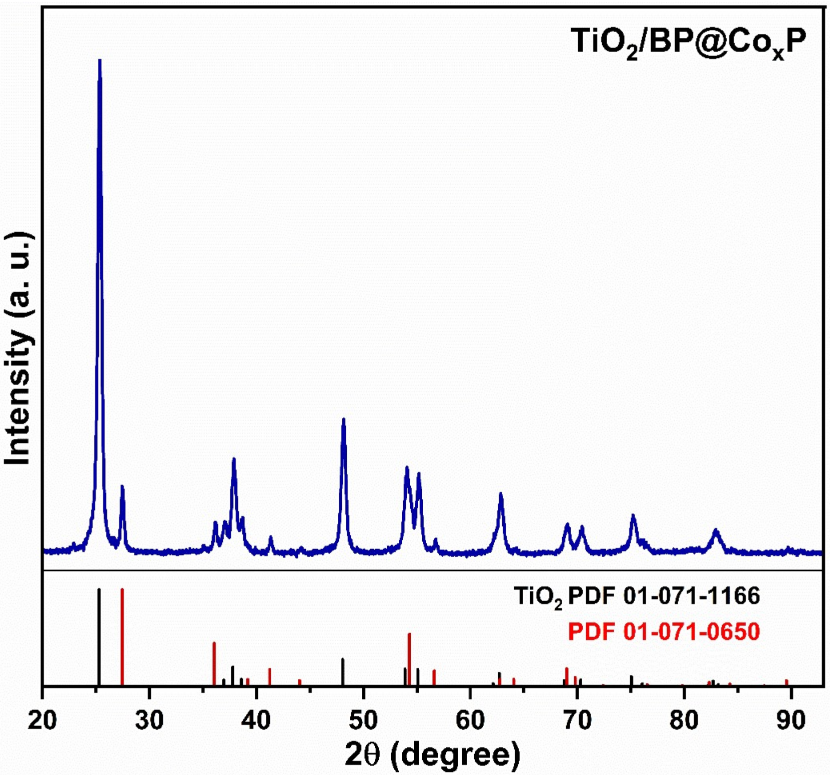

Figure S2. PXRD of TiO_2/BP@Co_xP with PDF card of TiO_2 having anatase and rutile.

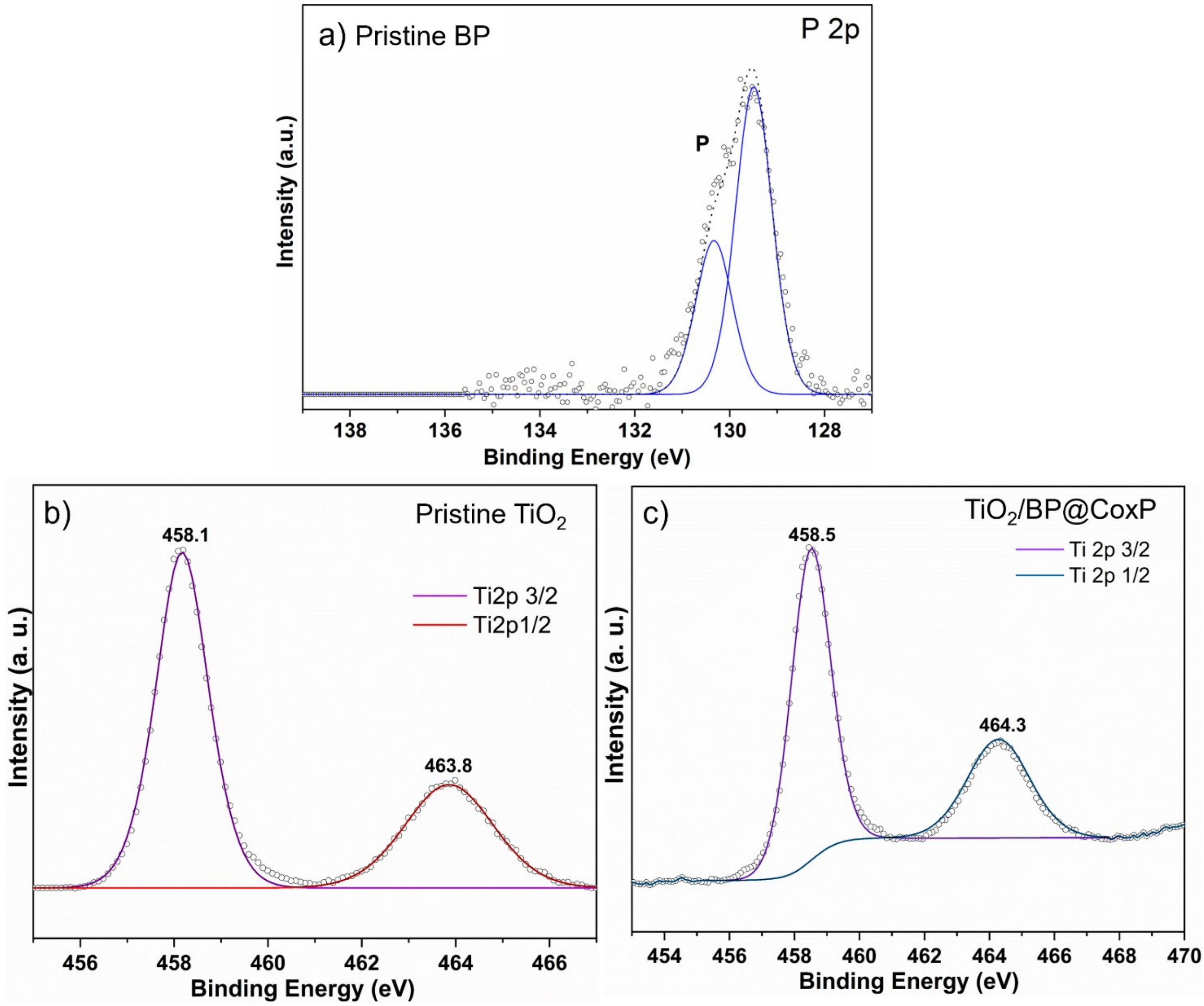

Figure S3. a)XPS P 2p core level spectrum of elemental black phosphorus. Ti 2p core level spectrum of b) pristine TiO_2 and c) TiO_2/BP@Co_xP.

Table S1. Results of the quantitative EXAFS analysis. The error on the last digit is shown in parenthesis.

	Co-P			Co-Co		
Sample	**N**	**R(A)**	**$\sigma^2(A^2)$**	**N**	**R(A)**	**$\sigma^2(A^2)$**
BP@CoPx	3.8(8)	2.23(2)	0.011(3)	0.8(7)	2.98(4)	0.01(1)
TiO_2/BP@CoPx	4(1)	2.24(3)	0.011(5)	1.1(7)	3.00(6)	0.02(2)
BP@CoPx aged	4(1)	2.25(2)	0.01(13)	1.3(7)	3.02(4)	0.01(1)
CoP	3.8 (8)	2.33(2)	0.011(3)	-	-	-
$Co(PPh_3)_3Cl$	4.1(5)	2.26(2)	0.006(1)	-	-	-
$Co(PPh_3)_2Cl_2$	4.4(6)	2.29(2)	0.008(2)	-	-	-

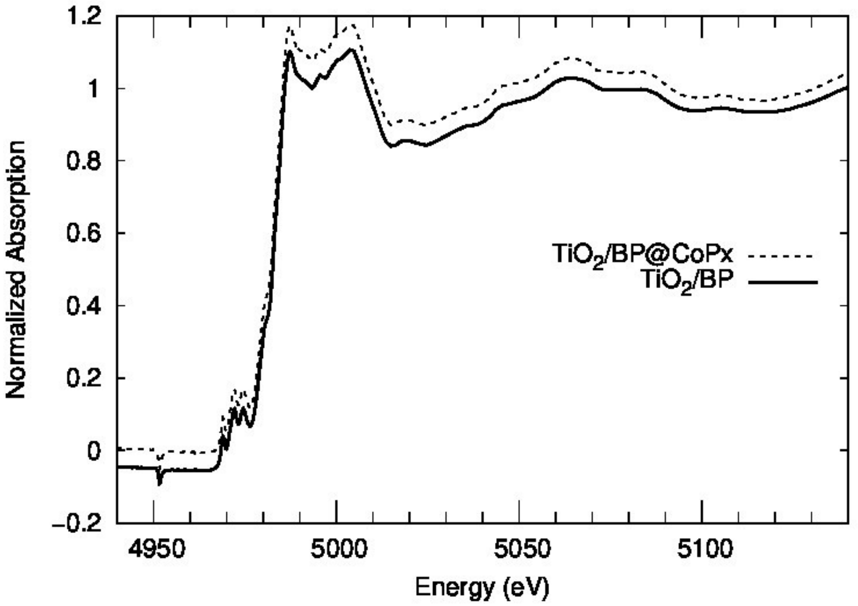

Figure S4. Ti-K edge XANES spectra of TiO_2/BP and TiO_2/BP@CoPx. The two spectra are slightly shifted vertically for clarity.

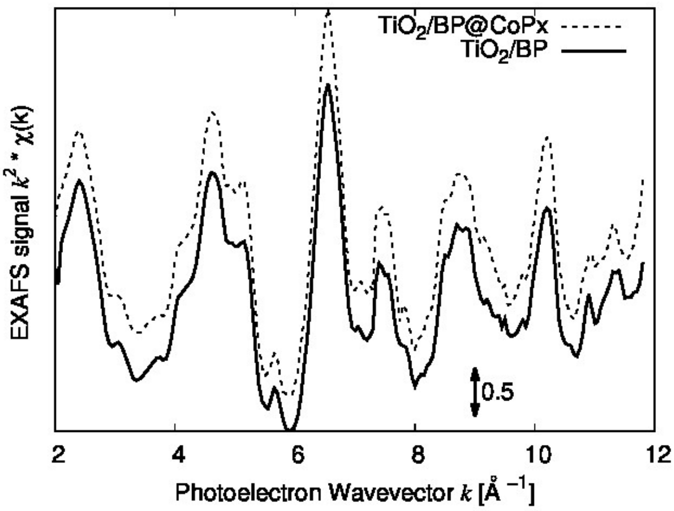

Figure S5. Ti-K edge EXAFS spectra of TiO_2/BP and TiO_2/BP@CoPx.

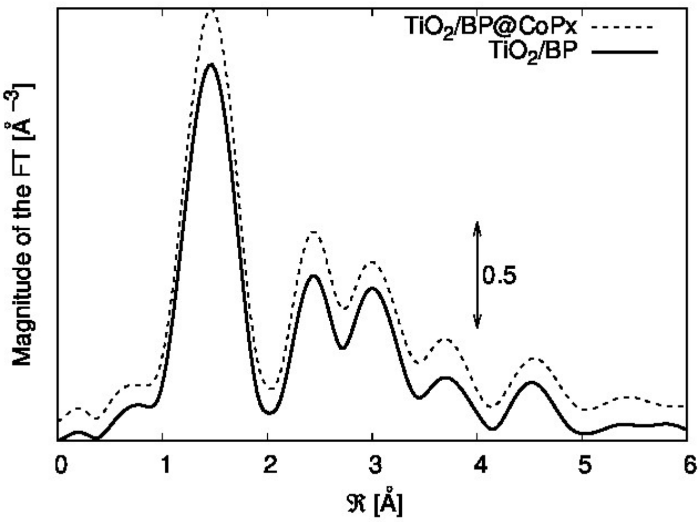

Figure S6. Fourier transforms (FT) of the EXAFS spectra shown in Fig. S5 and related fits.

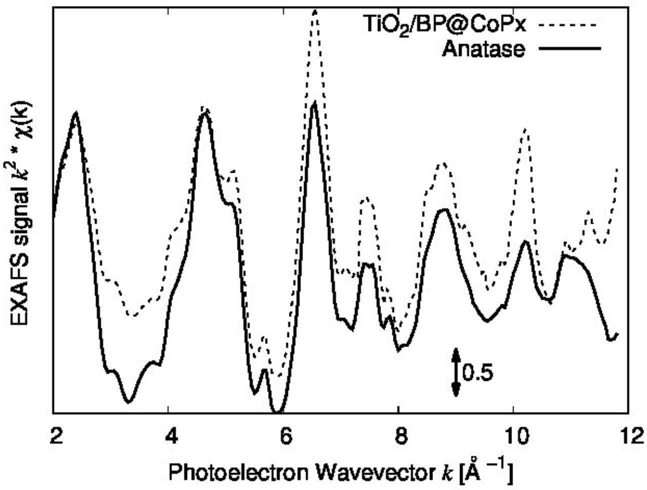

Figure S7. EXAFS data of TiO_2/BP@CoPx at Ti-K edge compared with anatase.

Table S2. Results of the quantitative EXAFS analysis at the Ti-K edge. The coordination numbers were kept at the crystallographic value and a common amplitude reduction s_0^2 =0.8(1) was found.

Parameter	**TiO_2/BP@CoxP**	**Anatase**
R_{O1} (Å)	1.92(2)	1.92(2)
$\sigma^2{}_{O1}$ (Å^2)	0.007(3)	0.007(2)
R_{O2} (Å)	1.96(2)	1.96(2)
$\sigma^2{}_{O2}$ (Å^2)	0.0005(5)	0.0002(2)
R_{Ti1} (Å)	3.06(4)	3.06(2)
$\sigma^2{}_{Ti1}$ (Å^2)	0.006(3)	0.006(1)
R_{Ti2} (Å)	3.80(4)	3.80 (2)
$\sigma^2{}_{Ti2}$ (Å^2)	0.010(5)	0.010(2)

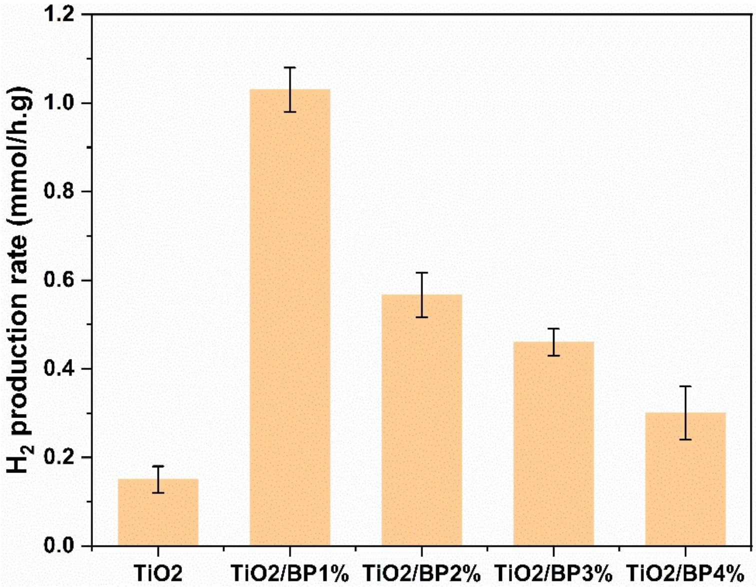

Figure S8. Comparison of HER using different wt% of BP loaded on TiO_2 under UV-Vis irradiation.

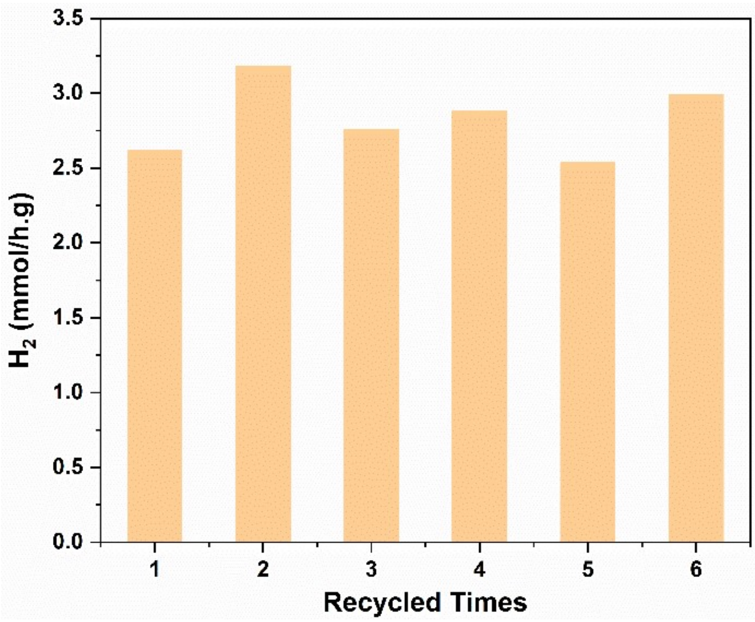

Figure S9. Stability test for $TiO_2/BP_{2\%}@Co_xP_{0.4\%}$.

a)

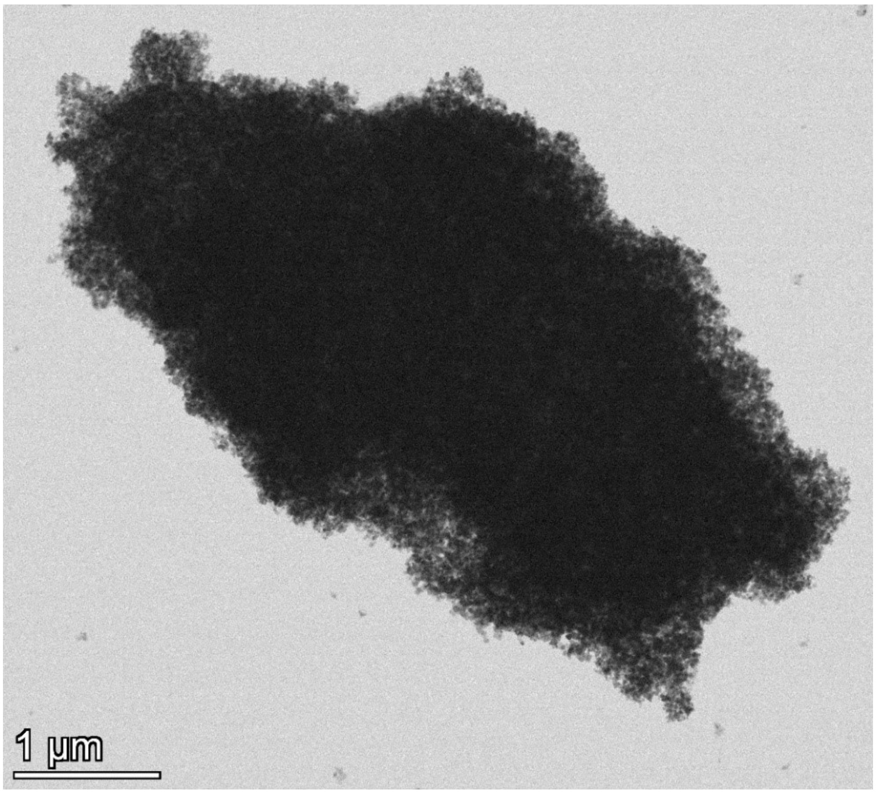

b)

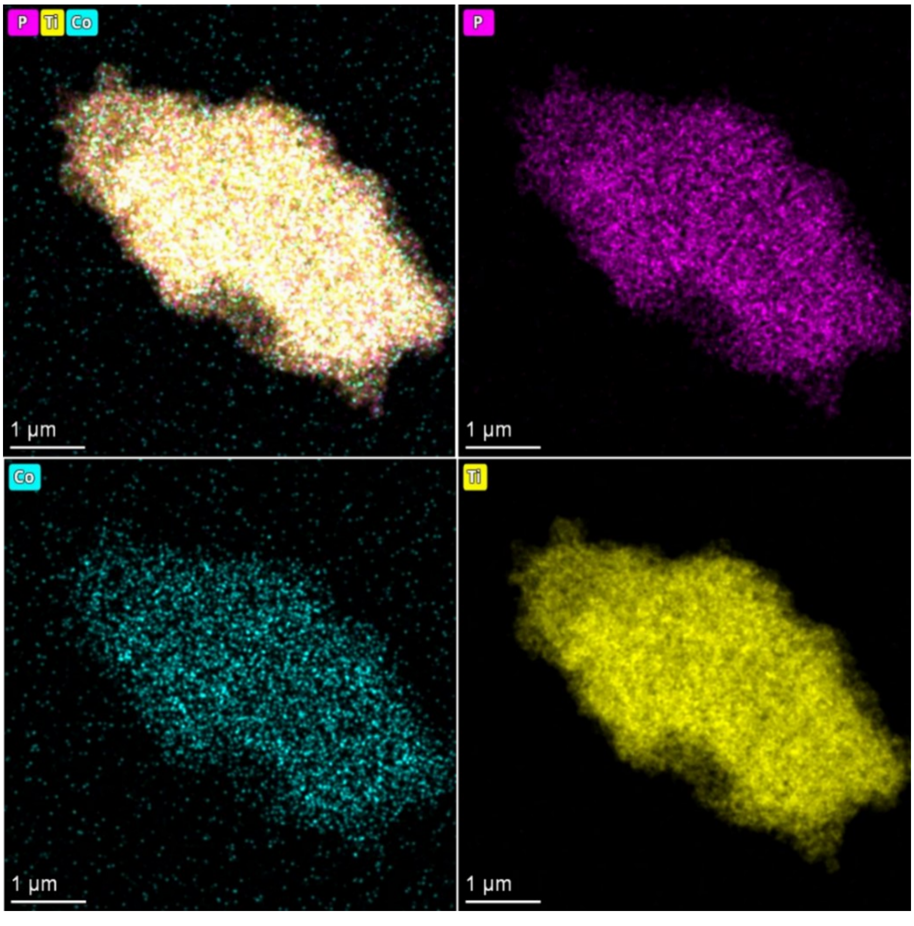

Figure S10. a) BF STEM and b) EDS mapping of TiO_2/BP@Co_xP recovered after recycling.

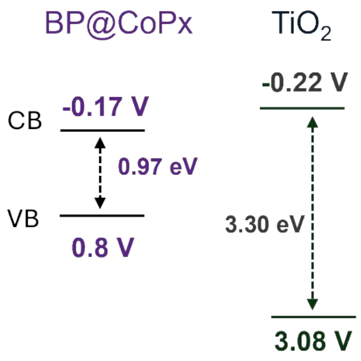

Figure S11. Band structure with energy levels before contact.

Table S3. Comparison of photocatalytic activity of similar titanium dioxide-based catalyst in hydrogen evolution.

Photocatalyst	Co-catalyst amount(wt%)	Sacrificial electron donor	H_2 evolution (mmol/g*h)	Reference
$TiO_2/BP_{2.5wt\%}$	Pt (3%)	TEOA (10 vol%)	2.0	1
Mesocrystal TiO_2/BP NS	Pt (3%)	MeOH (25% vol)	9.1 (solar light, 2sun)	2
sea urchin-like TiO_2/BPQDs	-	MeOH (16.6% vol)	0.112 (UV-Vis)	3
$TiO_2/BP_{1\%}$-$CoP_{2\%}$		MeOH (20% vol)	7.4 (300 W Xenon, UV-Vis, 1.4 sun)	4
$CdS/(BP\text{-}Co)_{1\%}$	-	Lactic acid (20 vol%)	17.2 (300 W Xenon, vis region)	5
BP-Co_2P NPs (3.3%wt)	-	0.1 M Na_2S/0.1 M Na_2SO_3	1.12 (300 W Xenon, vis region)	6
$TiO_2/BP_{2\%}$-$CoxP_{0.8\%}$	-	MeOH (20% vol)	**5.3** (300 W Xenon, UV-	This work

			Vis, 1.4 sun)	
BP-CoP NPs	-	Oxalic acid	0.694 (Vis-NIR)	7
BP-Co_xP NPs	-	MeOH (20% vol)	0.48 (300 W Xenon, vis region)	8
TiO_2-$CoP_{x\ (0.5\ wt\%)}$	-	MeOH (20% vol)	0.82 (AM 1.5G)	9

Table S4. Extracted fitting parameters from the equivalent circuit fitting.

Photocatalyst	*R_1 (Ohm)*	*R_2 (Ohm)*	*Q_2 [F.s^(n -1)]*	*n*
TiO_2	8.256	35024	56.12 e-6	0.944
BP	139.9	76634	2.083e-5	0.812
BP@CoxP	3.903	12502	8.768e-5	0.961
TiO_2/ BP@CoxP	25.61	4200	6.214e-5	0.864

Legend: R = resistance, Q = pseudocapacitance, n = exponent of the pseudocapacitance

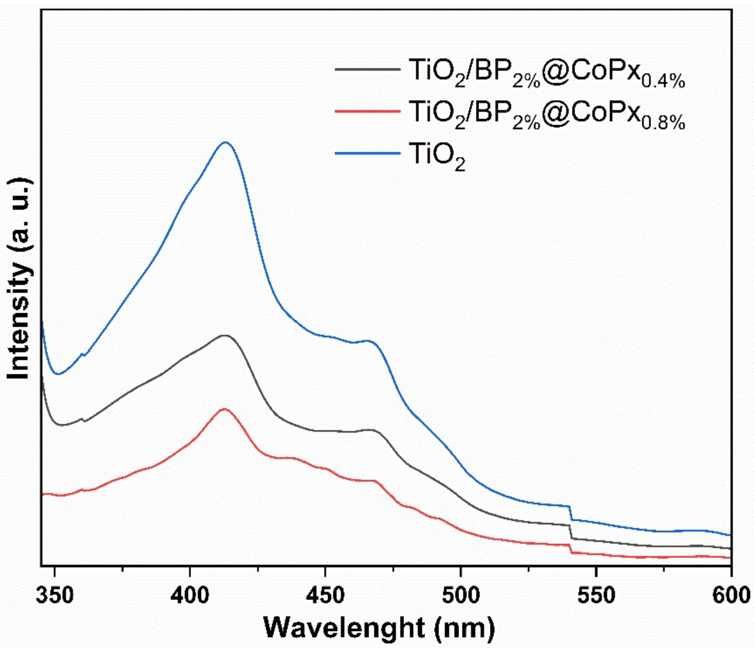

Figure S12. Steady-state photoluminescence performed at λ_{ex} = 325 nm.

1 J. Wu, S. Huang, Z. Jin, J. Chen, L. Hu, Y. Long, J. Lu, S. Ruan and Y.-J. Zeng, *J. Mater. Sci.*, 2018, **53**, 16557–16566.
2 O. Elbanna, M. Zhu, M. Fujitsuka and T. Majima, *ACS Catal.*, 2019, **9**, 3618–3626.
3 R. Guan, L. Wang, D. Wang, K. Li, H. Tan, Y. Chen, X. Cheng, Z. Zhao, Q. Shang and Z. Sun, *Chem. Eng. J.*, 2022, **435**, 135138.
4 G. Provinciali, J. Filippi, A. Lavacchi, S. Caporali, M. Banchelli, M. Serrano-Ruiz, M. Peruzzini and M. Caporali, *ChemCatChem*, 2023, **15**, e202300647.
5 X. Ren, L. Shi, Y. Li, S. Song, Q. Wang, S. Luo, L. Ren, H. Zhang, Y. Izumi, X. Peng, D. Philo, F. Ichihara and J. Ye, *ChemCatChem*, 2020, **12**, 3870–3879.
6 Y.-J. Yuan, Z.-K. Shen, S. Song, J. Guan, L. Bao, L. Pei, Y. Su, S. Wu, W. Bai, Z.-T. Yu, Z. Ji and Z. Zou, *ACS Catal.*, 2019, **9**, 7801–7807.
7 Q. Liang, F. Shi, X. Xiao, X. Wu, K. Huang and S. Feng, *ChemCatChem*, 2018, **10**, 2179–2183.
8 A. Ozawa, M. Yamamoto, T. Tanabe, S. Hosokawa and T. Yoshida, *J. Mater. Chem. A*, 2020, **8**, 7368–7376.
9 R. Liang, Y. Wang, C. Qin, X. Chen, Z. Ye and L. Zhu, *Langmuir*, 2021, **37**, 3321–3330.